DOE/SC-ASR-11-004

FY 2011 4th Quarter Metric Estimate of Future Aerosol Direct and Indirect Effects

September 2011

U.S. DEPARTMENT OF ENERGY
Office of Science

ASR
Atmospheric System Research

DISCLAIMER

DOE/SC-ASR-11-004

FY 2011 4th Quarter Metric Estimate of Future Aerosol Direct and Indirect Effects

September 2011

Work supported by the U.S. Department of Energy,
Office of Science, Office of Biological and Environmental Research

Contents

Figures

1.0 Introduction

The global and annual mean aerosol direct and indirect effects, relative to 1850 conditions, estimated from CESM simulations are 0.02 W m^{-2} and -0.39 W m^{-2}, respectively, for emissions in year 2100 under the IPCC RCP8.5 scenario. The indirect effect is much smaller than that for 2000 emissions because of much smaller SO_2 emissions in 2100; the direct effects are small due to compensation between warming by black carbon and cooling by sulfate.

These estimates are based on the following considerations.

Aerosol particles influence climate through a variety of mechanisms: (1) by scattering, absorbing, and emitting radiant energy in the atmosphere and at the surface when deposited on snow and ice; (2) by serving as the nuclei for droplet and ice crystal formation in clouds, and (3) by influencing the biogeochemical cycles through fertilization and acidification of soil, lakes, and the ocean.

The term *aerosol direct effects* refers to the direct impact of anthropogenic aerosol particles on the planetary energy balance through scattering, absorption, and emission of radiation in the atmosphere, without consideration of the aerosol effects of the radiative heating on clouds. The term *aerosol indirect effect* refers to the impact through the influence of anthropogenic aerosol on the optical properties of clouds by serving as the nuclei for droplets and ice crystals. The anthropogenic aerosol can change droplet and ice crystal number concentration, influencing cloud particle surface area, droplet collisions, the accumulation of liquid water and ice in clouds, and even cloud dynamics, cloud lifetime, and cloud amount, all of which change the reflectivity and emissivity of clouds and precipitation.

These aerosol effects are important to the Earth system. Efforts to quantify aerosol direct and indirect effects between preindustrial and present day conditions suggest a radiative cooling that is nearly as large as the radiative warming due to anthropogenic increases in CO_2, but large uncertainties remain. These uncertainties confound interpretation of climate change due to CO_2 increases between pre-industrial and present times and limit our ability to project future climate change. Changes in future emissions of aerosols and their precursor gases could contribute to future climate change in ways that have not been quantified.

Aerosol direct effects have been treated in climate models for at least 10 years, but aerosol indirect effects have only recently been added to climate models. The CESM is one such model with a treatment of aerosol indirect effects. With support from the Department of Energy Atmospheric System Research (ASR) and Scientific Discoveries through Advanced Computing (SciDAC) programs, an advanced representation of the aerosol life cycle and aerosol direct and indirect effects has been incorporated within the CESM as part of version 5.1 of the Community Atmospheric Model (CAM5.1, Rasch et al 2011). Other versions of CAM use simpler treatments of aerosols that do not include many of the aerosol processes described below.

CAM5.1 uses a “modal” treatment (Liu et al 2011a). All important aerosol sources (natural as well as anthropogenic) are included. The aerosol size distribution is expressed in terms of three log-normal modes, each composed of an internal mixture of all of the important aerosol components (sulfate, black carbon, organic carbon, sea salt, and mineral dust), with number as well as mass concentration simulated for each mode. Aerosol processes represented in the model include emissions of primary particles and

precursor gases; oxidation of the precursor gases; new particle formation; particle growth by condensation; particle coagulation; transport by resolved winds, turbulence, and convective clouds; growth by humidification; activation to form cloud droplets and ice crystals; aqueous-phase chemistry; nucleation and impaction scavenging; and dry deposition to the surface.

The treatment of the optical properties of each aerosol mode (Ghan and Zaveri 2007) accounts for humidification effects, size dependence, and internal mixing of the aerosol components with water, which is important for treating absorption by black carbon when it is coated with sulfate, organic, and water. Aerosol direct effects are calculated by differencing radiative transfer calculations with and without aerosols.

Aerosol indirect effects are treated using a double moment cloud microphysics scheme (Morrison and Gettelman 2008, Gettelman et al. 2008). Droplet nucleation is related to properties of all of the aerosol modes (Abdul-Razzak and Ghan 2000). Ice crystals form by homogeneous nucleation on sulfate particles and heterogeneous nucleation on dust particles (Liu and Penner 2005, Liu et al. 2007, Gettelman et al. 2010). Droplet number influences liquid water content and precipitation through its influence on the autoconversion process. Cloud optical properties depend on droplet and crystal number as well as liquid and ice water path, which together produce the aerosol indirect effect.

To estimate aerosol indirect effects, it is necessary to isolate aerosol effects on clouds from other influences on clouds. This is typically accomplished by changing aerosol emissions while holding constant the greenhouse gas concentrations, sea surface temperature, and sea ice. Recent work also suggests that it is helpful to constrain the winds by nudging simulated winds toward observed winds. Direct and indirect effects can then be estimated from the simulated changes Δ in the radiative flux at the top of the atmosphere (between two climate states having different aerosol distributions), written as a statement of identity with two separate terms:

$$\Delta F = \Delta(F - F_{no\_aer}) + \Delta F_{no\_aer} \quad (1)$$

where F is the radiative flux from the simulation and F_{no_aer} is the radiative flux separately calculated by neglecting all scattering, absorption and emission of radiation by the aerosols. The first term in (1) represents the direct effects of the changes in the aerosol due to changes in emissions. The difference F-F_{no_aer} is the direct radiative effect of all of the aerosol, accounting for the dependence on the distributions of clouds as well as the aerosol. The change $\Delta(F\text{-}F_{no\_aer})$ thus quantifies the change of the direct effect. Note that changes in clouds will affect both F and F_{no_aer} in similar ways, so the first term is insensitive to changes in clouds.

Since equation (1) is just a statement of identity, the second term in (1) simply completes the identity. However, because F_{no_aer} neglects the direct influence of aerosols on the radiative flux, ΔF_{no_aer} is only directly influenced by changes in clouds or in the surface temperature and reflectivity. If sea surface temperature and sea ice are constant, changes in surface temperature and reflectivity are small, and changes in clouds are entirely due to changes in the aerosol. The cloud changes can be considered to be the indirect effect, although the term also includes the radiative effects of cloud changes induced by radiative absorption, scattering and emission from changes in the aerosol (known as the semi-direct effect). Isolating the semi-direct effect from the indirect effect would require a separate simulation that neglects radiative absorption, scattering and emission by the aerosol. Since the semi-direct effect is usually much smaller than the indirect effect, the distinction is often neglected, so the second term in

(1) could be considered a measure of aerosol indirect effects. In this report we will call the second term aerosol indirect effects, although we acknowledge that some of the signal is due to semi-direct effects that have not been quantified for the CESM.

Although it is possible to estimate aerosol direct and indirect effects continuously as emissions change (Takemura et al. 2006), the effects are more commonly estimated by contrasting two different emissions scenarios. We have done the latter.

We report here on changes in aerosol forcing between pre-industrial, present day (year 2000), and projected future emissions for year 2100. Three six-year simulations by the CESM were performed using present-day (year 2000) ocean surface conditions (sea surface temperature and sea ice) and oxidant (O_3, OH, NO_3, HO_2) concentrations, one with preindustrial (year 1850) emissions of primary aerosol (organic carbon, black carbon, and SO_4) and aerosol precursor gases (SO_2, volatile organic compound); one present-day (year 2000) emissions of aerosol and precursor gases; and one with future (year 2100) emissions. For the year 2100 we use the IPCC Representative Concentration Pathways (RCP) 8.5 emissions scenario, which is estimated to produce an 8.5 W m^{-2} radiative forcing by greenhouse gases and aerosols together (Moss et al. 2010). Direct and indirect solar effects of anthropogenic aerosol for present day and future emissions are estimated from the difference Δ with respect to the preindustrial simulation. Direct effects for longwave radiation are assumed to be negligible, while indirect longwave effects are estimated from the difference in the longwave cloud forcing rather than F_{no_aer} so that changes in clear sky longwave due to changes in land surface temperature do not produce a spurious indirect longwave effect.

In this report we compare the radiative forcing for year 2100 with that for 2000. The differences in the forcing are driven by differences in emissions, which are taken from IPCC (Lamarque et al. 2010, Moss et al. 2010). The global mean emissions for years 1850, 2000, and 2100 are illustrated in Figure 1. SO_2 emissions decrease from about 130 Tg/yr in 2000 to about 50 Tg/yr in 2100 for the RCP8.5 scenario as sulfur scrubbers are added to coal power plants. Emissions of black carbon are reduced too, but much less, from 7.8 Tg/yr to 4.4 Tg/yr.

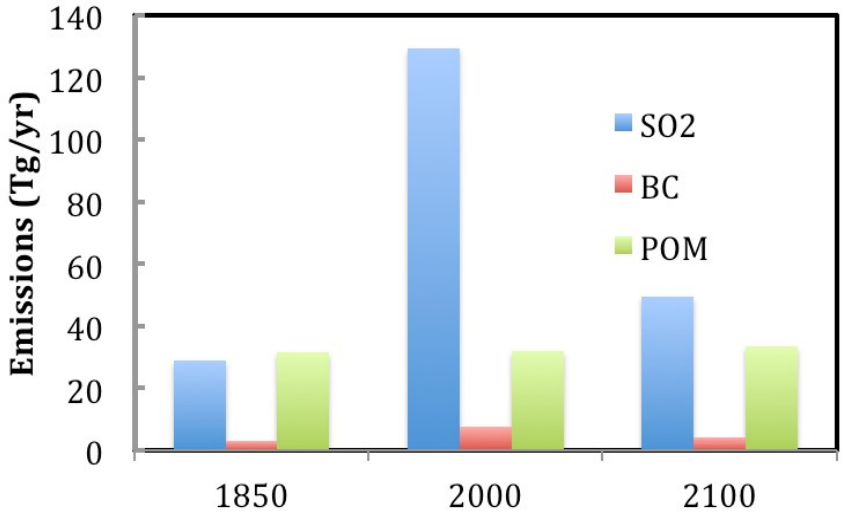

Figure 1. Global annual emissions.

Figure 2 compares the global mean solar direct and indirect aerosol radiative forcing and longwave indirect forcing for years 2000 and 2100. The direct forcing is small for both 2000 and 2100 emissions (due to cancellation of cooling by sulfate and organic carbon and warming by black carbon) but is slightly more positive for 2100 because of the larger relative reductions in sulfur emissions compared with reductions in black carbon emissions. The indirect solar forcing is more than a factor of three smaller for 2100 as SO_2 emissions are also smaller by a factor of more than two. The indirect longwave forcing is smaller by a factor of almost three. The total aerosol radiative forcing is smaller by a factor of four.

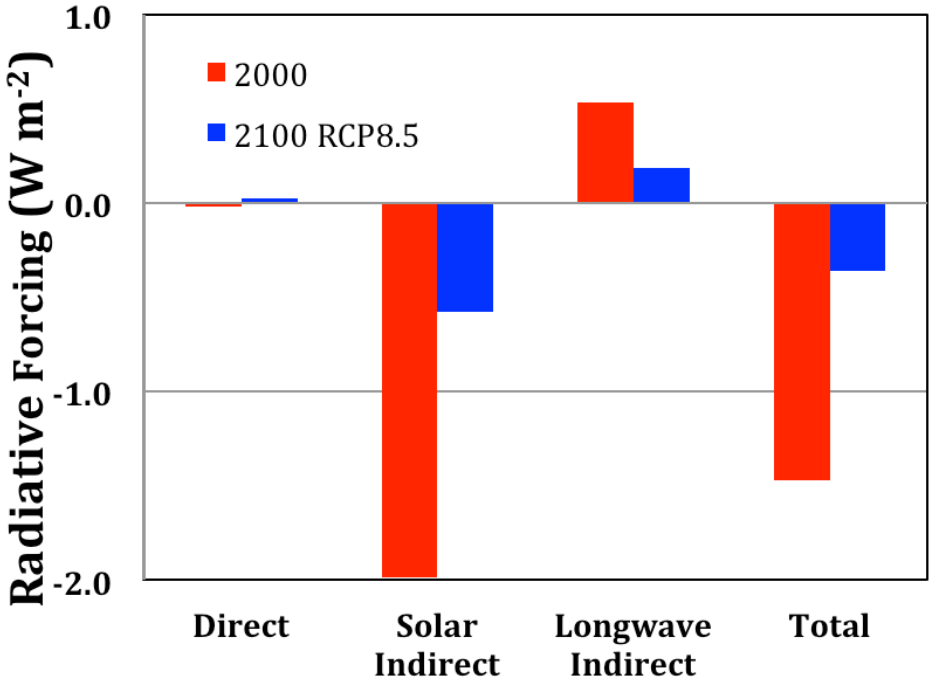

Figure 2. Global annual mean direct and indirect aerosol radiative forcing with respect to 1850 emissions for emissions for year 2000 and for the IPCC RCP 8.5 scenario for year 2100, as estimated by CAM5.1

Figure 3 compares the spatial distribution of the annual mean direct effects for 2000 and 2100. Regions with positive and negative forcing are evident for both cases. Negative forcing occurs when anthropogenic sulfate aerosol, which mainly scatters solar radiation, accumulates over the ice-free and cloud-free ocean, which is relatively dark. The radiative cooling is most evident over the Mediterranean Sea but is also evident over the subtropical Atlantic, Pacific, and Indian oceans. The radiative cooling is much weaker for year 2100 than 2000 due to the large reduction in emissions of SO_2.

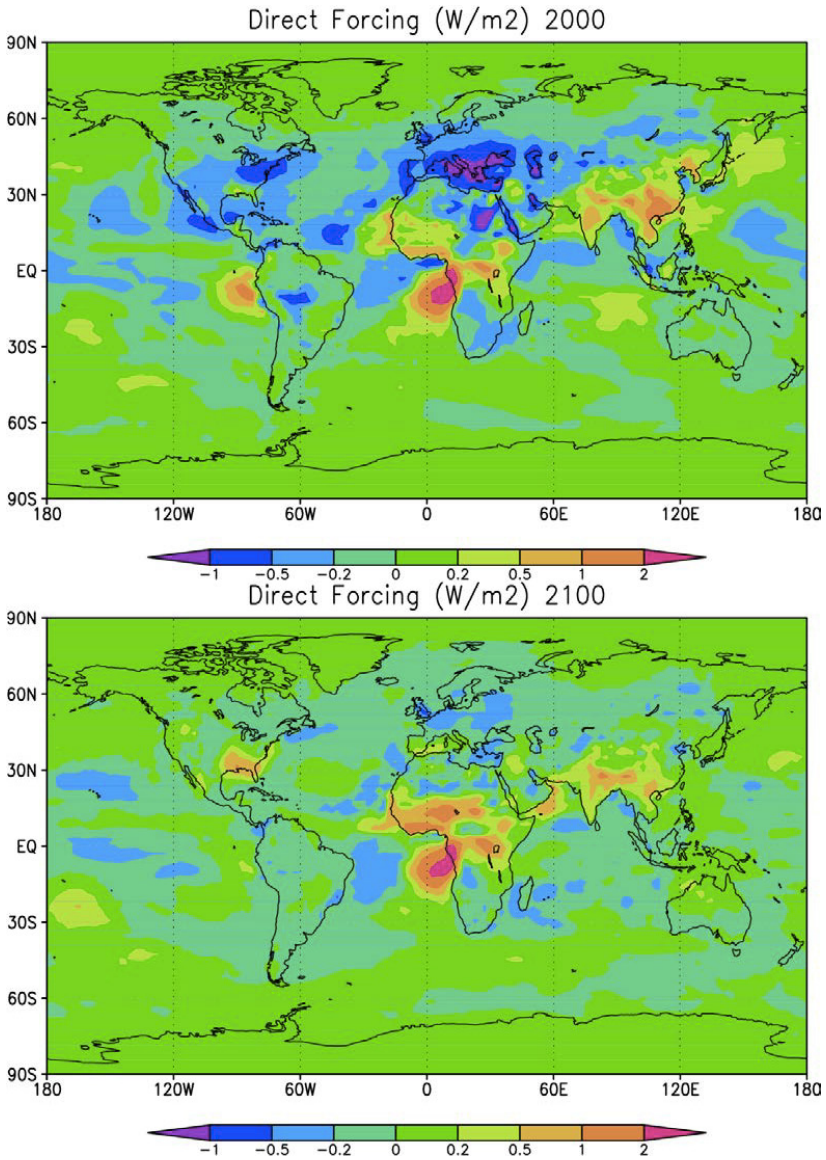

Figure 3. The annual mean direct forcing by anthropogenic aerosol at the top of the atmosphere for years 2000 (above) and 2100 (below).

Positive direct forcing occurs when black carbon accumulates above a bright surface or clouds. Although some radiative warming is simulated over the snow and sea ice in polar regions, the black carbon burdens are relatively low there and are accompanied by sulfate and organic carbon (which primarily scatter). Since the incoming solar energy is low or zero when the burdens are greatest during the winter months, the radiative forcing there is weak. The strongest radiative warming is found near the biomass burning regions in Africa, when smoke is transported over clouds (Chand et al. 2009). Large positive forcing is also simulated over eastern China, which suggests significant black carbon is transported above clouds, and off the equatorial west coast of South America, where smoke from Amazon fires is transported over clouds there. A larger warming is estimated in sub-Saharan Africa in 2100 than 2000 due to increased biomass burning in 2100. The warming in east China is lower in 2100 than 2000 due to reduced black carbon emissions. The strong negative forcing seen over the northeast U. S., Europe, and the Amazon is substantially reduced.

The spatial distributions of the annual shortwave indirect forcing, shown in Figure 4, are quite different for 2000 and 2100 emissions. Figure 4 shows the spatial distribution of the annual mean shortwave indirect effect. Strong indirect negative forcing is simulated over south Asia for 2000 emissions. For 2100 emissions, the forcing over south Asia is weaker, and stronger positive forcing is simulated over the eastern U.S. and western Europe. The differences are largely due to differences in the simulated change in cloud liquid water path, shown in Figure 5. Liquid water path increases in south Asia in 2100 and decreases in the eastern U. S. and Europe in 2100. The latter can be explained by the simulated change in cloud condensation nuclei concentration (CCN) (Figure 6), which increases across much of the northern hemisphere in 2000, but increases only over south Asia (less than in 2000) and Africa in 2100. CCN concentration decreases over the eastern U.S. and western Europe due to reductions in biomass and coal burning since 1850, so the decrease in liquid water path in 2100 is due to associated decreases in droplet number and hence initiation of precipitation at lower liquid water concentration.

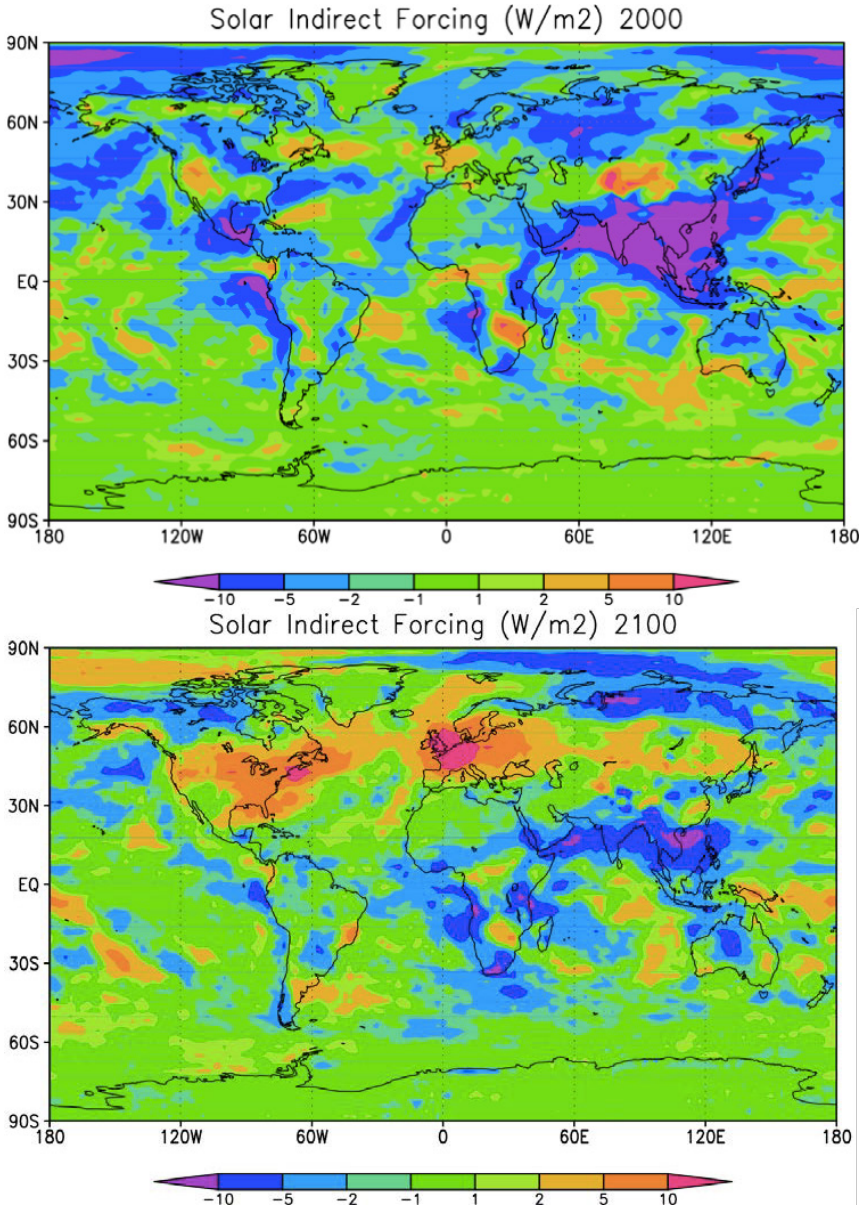

Figure 4. Annual mean solar indirect forcing for years 2000 and 2100.

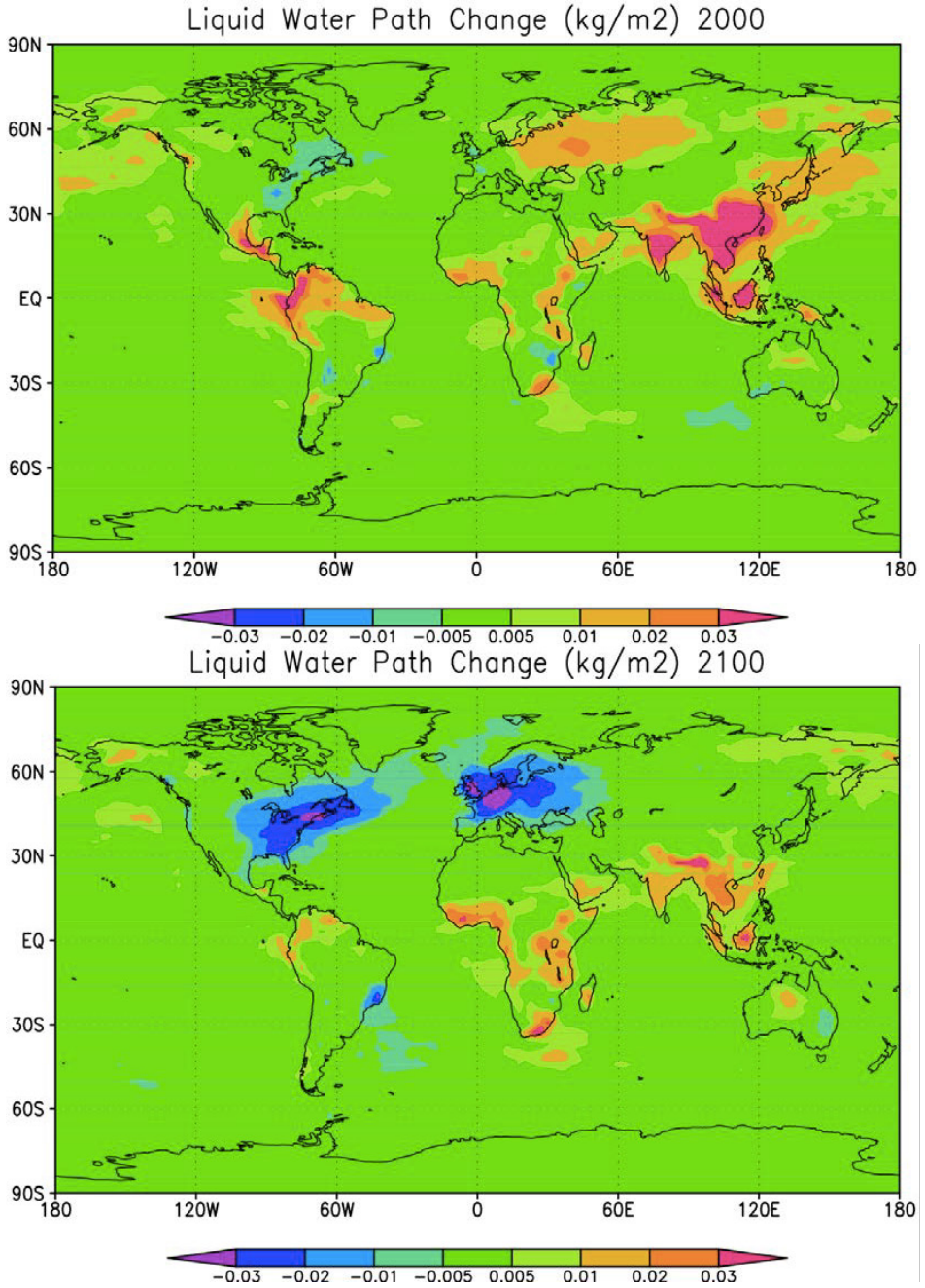

Figure 5. Annual mean change in liquid water path for years 2000 and 2100.

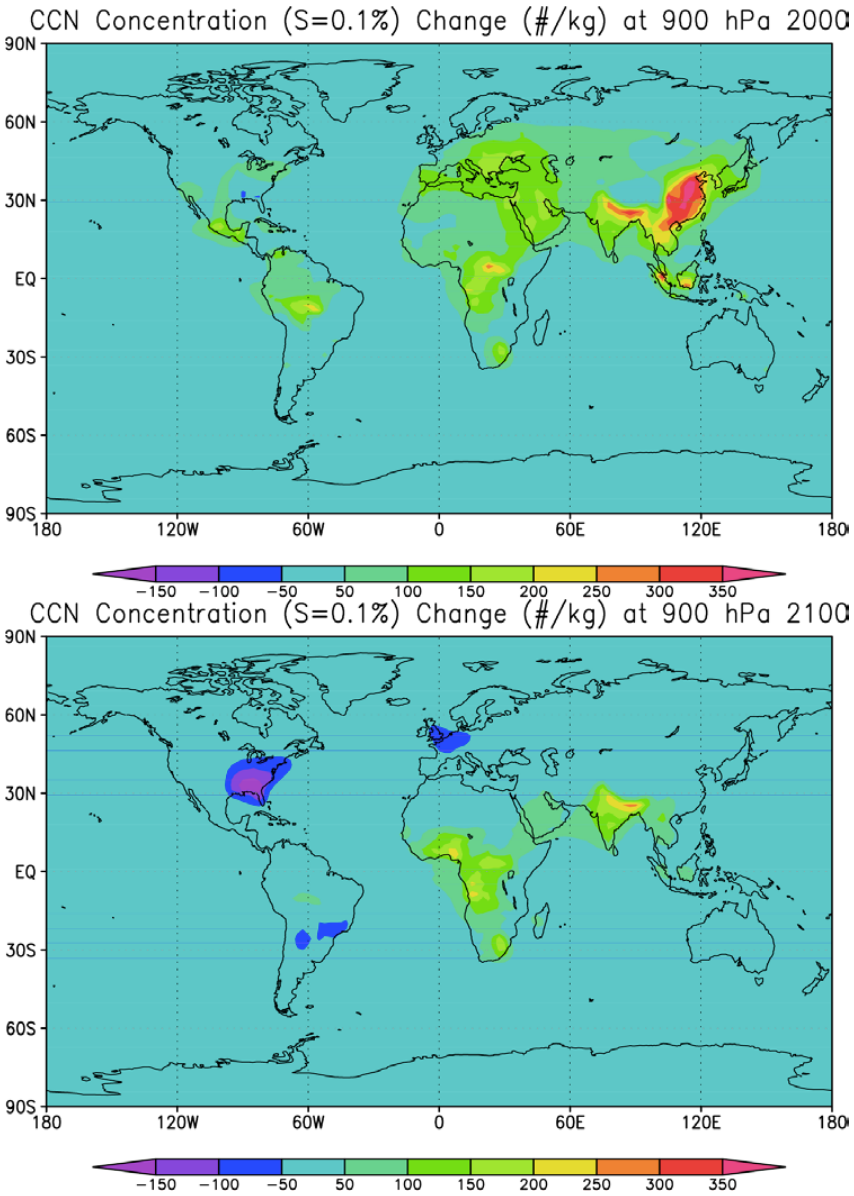

Figure 6. Change in CCN concentration (with respect to 1850 conditions) at 1% supersaturation and 900 hPA for years 2000 and 2100.

Most previous estimates of aerosol indirect effects have focused on effects on solar radiation. The CESM produces surprisingly strong aerosol indirect effects on longwave radiation. The longwave indirect effect is estimated differently from the shortwave because the changes in simulated land temperature produce a significant change in the longwave flux at the top of the atmosphere that is a signature of the response rather than the forcing. Since we want to know the forcing rather than the response, we estimate the longwave indirect effect from the change in the longwave cloud forcing, $\Delta(F\text{-}F_{clear})$. Figure 7 shows the spatial distribution of the annual mean of this estimate. Positive forcing exceeding 5 Wm^{-2} is simulated for 2000 in a wide swath from Arabia to the subtropical northwest Pacific Ocean, and radiative cooling is simulated over west Africa and parts of South America. Consistent with the smaller aerosol concentrations in 2100 than in 2000, the longwave indirect forcing is generally smaller for 2100 emissions.

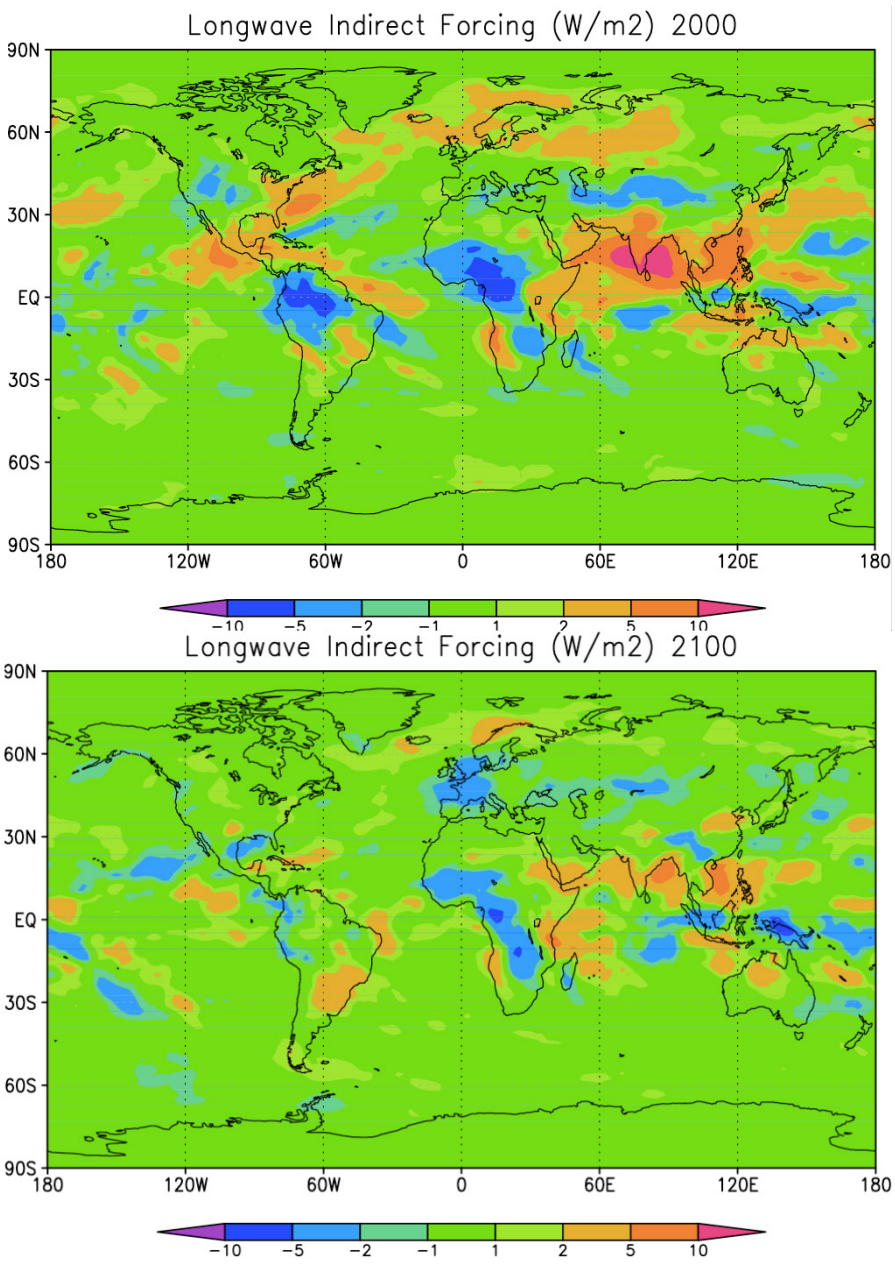

Figure 7. Annual mean longwave indirect forcing for 2000 and 2100.

What is causing the longwave cloud response? Figure 8 shows the change in crystal number concentration at 200 hPa for 2000 and 2100. The longwave indirect forcing is strongly correlated with changes in upper troposphere crystal number concentration and resulting changes in cloud ice mixing ratio and cloud fraction. The changes in crystal number reflect changes in both deep convection (which increases in some places and decreases in other places) and droplet nuclei concentration (which increases everywhere, albeit by varying degrees). The weaker change in 2100 is consistent with the smaller increase in upper tropospheric CCN concentration in 2100, shown in Figure 9. Since none of the anthropogenic aerosol in CAM5 is treated as heterogeneous ice nuclei, the correlation of the CCN and crystal number changes suggests that enhanced homogeneous nucleation (droplet freezing) is the mechanism for the upper tropospheric changes in cloud.

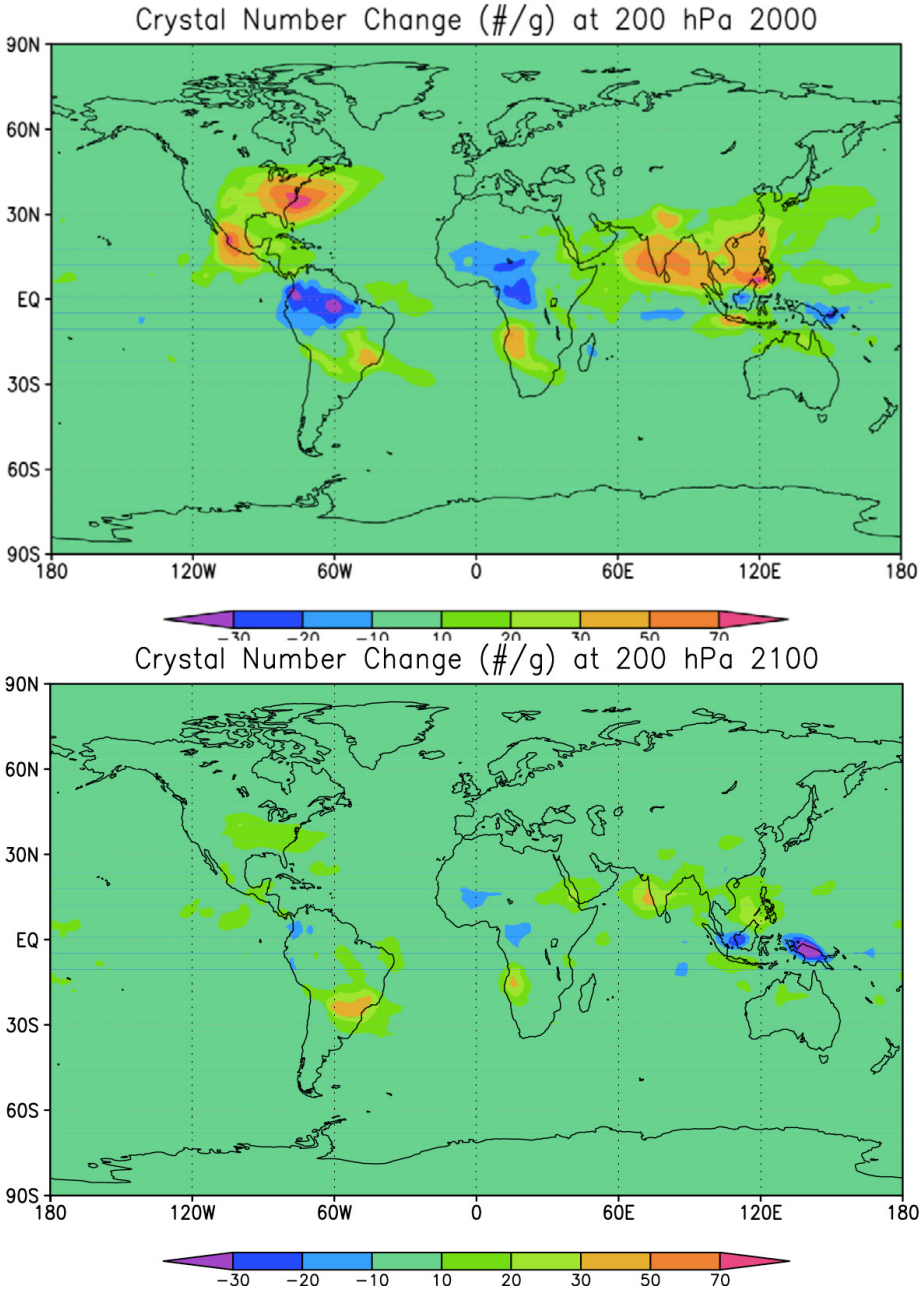

Figure 8. Change in annual mean ice crystal number concentration at 200 hPa.

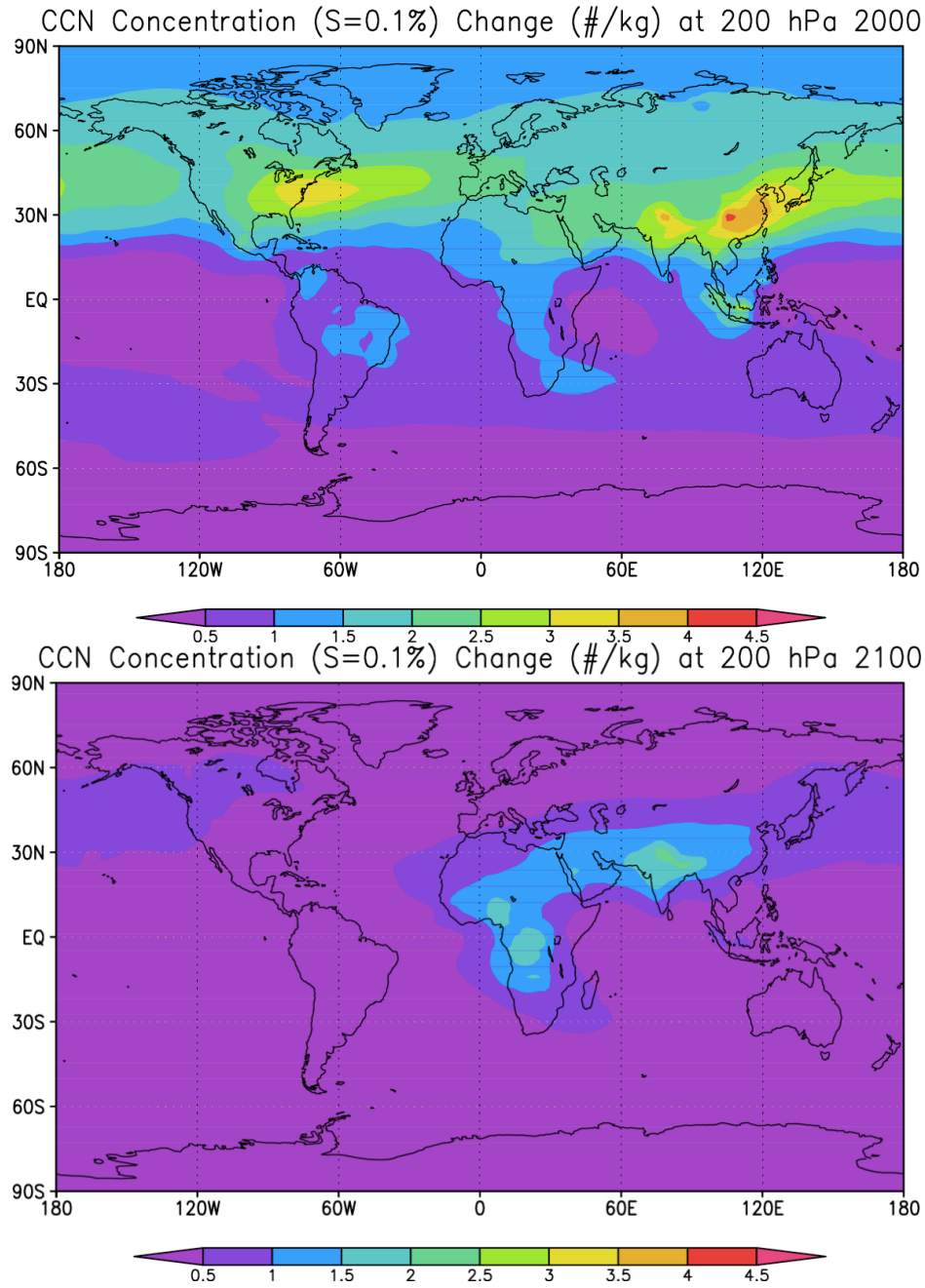

Figure 9. Change in annual mean CCN concentration at 200 hPa for 2000 and 2100 emissions.

This work and much more is described in a manuscript being prepared for publication (Liu et al. 2011b).

2.0 References

Abdul-Razzak, H, and SJ Ghan. 2000. "A parameterization of aerosol activation. Part 2: Multiple aerosol types." *Journal of Geophysical Research* 105: 6837–6844.

Chand, D, R Wood, TL Anderson, SK Satheesh, and RJ Charlson. 2009. "Satellite- derived direct radiative effect of aerosols dependent on cloud cover." *Nature* Geoscience 2: 181–184, doi:10.1038/NGEO437.

Gettelman, A, H Morrison, and SJ Ghan. 2008. "A new two-moment bulk stratiform cloud microphysics scheme in the NCAR Community Atmosphere Model (CAM3), Part II: Single-column and global results." *Journal of Climate* 21: 3660–3679.

Gettelman, A, X Liu, SJ Ghan, H Morrison, S Park, A Conley, SA Klein, J Boyle, D Mitchell, and J-L F Li. 2010. "Global simulations of ice nucleation and ice supersaturation with an improved cloud scheme in the community atmosphere model." *Journal of Geophysical Research* 115(D18216): doi:10.1029/2009JD013797.

Ghan, SJ, and RA Zaveri. 2007. "Parameterization of optical properties for hydrated internally-mixed aerosol." *Journal of Geophysical Research* 112: D10201, doi:10.1029/2006JD007927.

Lamarque, JF, et al. 2010. "Historical (1850–2000) gridded anthropogenic and biomass burning emissions of reactive gases and aerosols: methodology and application." *Atmospheric Chemistry and Physics* 10: 7017–7039, doi:10.5194/acp-10-7017-2010.

Liu, X, JE Penner, SJ Ghan and M Wang. 2007. "Inclusion of ice microphysics in the NCAR community atmospheric model version 3 (CAM3)." *Journal of Climate* 20(18): 4526–4547, doi:10.1175/Jcli4264.1.

Liu, XH, and JE Penner. 2005. "Ice nucleation parameterization for global models." *Meteorologische Zeitschrift* 14(4): 499–514, doi10.1127/0941-2948/2005/0059.

Liu, X, RC Easter, SJ Ghan, R Zaveri, P Rasch, J-F. Lamarque, A Gettelman, H Morrison, F Vitt, A Conley, S Park, R Neale, C Hannay, A Ekman, P Hess, N Mahowald, W Collins, M Iacono, M Flanner, and D Mitchell. 2011a. "Toward a minimal representation of aerosol direct and indirect effects: Model Description and Evaluation." *Geoscientific Model Development*, in preparation.

Liu, X, SJ Ghan, RC Easter, R Zaveri, P Rasch, and J-H. Yoon." 2011b. "Toward a minimal representation of aerosol direct and indirect effects: Model Description and Evaluation. Sensitivity and decomposition." *Journal of Climate*, in preparation.

Morrison, H, and A Gettelman. 2008. "A new two-moment bulk stratiform cloud microphysics scheme in the community atmosphere model, version 3 (CAM3). Part I: Description and numerical tests." *Journal of Climate* 21(15): 3642–3659, doi:10.1175/2008jcli2105.1.

Moss, RH, JA Edmonds, KA Hibbard, MR Manning, SK Rose, DP van Vuuren, TR Carter, S Emori, M Kainuma, T Kram, GA Meehl, JFB Mitchell, N Nakicenovic, K Riahi, SJ Smith, RJ Stouffer, AM Thomson, JP Weyant, and TJ Wilbanks. 2010. "The next generation of scenarios for climate change research and assessment." *Nature*, *463*, doi:10.1038/nature08823.

Rasch, PJ, R Neale, C Hannay, et al. 2011. "Version 5 of the Community Atmosphere Model (CAM5)." *Journal of Climate*, in preparation.

Takemura, T, Y Tsushima, T Yokohata, T Nozawa, T Nagashima, and T Nakajima. 2006. "Time evolutions of various radiative forcings for the past 150 years estimated by a general circulation model." *Geophysical Research Letters* 33*:* Ll9705, doi:10.1029/2006GL026666.